Imaging System Performance and Visibility as Affected by the Physical Environment

Grace Chang
Sea Engineering, Inc.
200 Washington St., Suite 210
Santa Cruz, CA 95060
Phone: (831) 421-0871 Fax: (831) 421-0875 Email: gchang@seaengineering.com

Award Number: N00014-11-M-0144

LONG-TERM GOALS

The long-term goal of "Imaging System Performance and Visibility as Affected by the Physical Environment" is to investigate the relationships between physical forcing and optical properties, including the imaging performance parameters. Our efforts are aimed at supporting the Radiance in a Dynamic Ocean (RaDyO) program, which is devoted to the topic of light propagation and imaging across the air-sea interface and within the surface boundary layer of natural water bodies. The primary goals of the RaDyO program are to:

1) Examine time-dependent oceanic radiance distribution in relation to dynamic surface boundary layer (SBL) processes.
2) Construct a radiance-based SBL model.
3) Validate the model with field observations.
4) Investigate the feasibility of inverting the model to yield SBL conditions.

OBJECTIVES

The objectives of this project are to:

1) Determine the relationships between physical processes and the optical properties that affect underwater visibility and the imaging performance parameters.
2) Year 2 Option: Investigate the effects of vertical variability (e.g., vertical layering) of optical properties on the image performance parameters, i.e. modulation transfer function (MTF) and point spread function (PSF).

We discuss the MTF of two different optical water types: (1) a dynamic, shallow-water, eutrophic environment and (2) a relatively clear, deep water, mesotrophic environment, and the relationships between the MTF and optical properties and physical processes (Chang and Twardowski, 2011).

Report Documentation Page

Form Approved
OMB No. 0704-0188

1. REPORT DATE	2. REPORT TYPE	3. DATES COVERED
30 SEP 2011		**00-00-2011 to 00-00-2011**

4. TITLE AND SUBTITLE	5a. CONTRACT NUMBER
Imaging System Performance and Visibility as Affected by the Physical Environment	5b. GRANT NUMBER
	5c. PROGRAM ELEMENT NUMBER
6. AUTHOR(S)	5d. PROJECT NUMBER
	5e. TASK NUMBER
	5f. WORK UNIT NUMBER
7. PERFORMING ORGANIZATION NAME(S) AND ADDRESS(ES) **Sea Engineering, Inc,200 Washington St., Suite 210,Santa Cruz,CA,95060**	8. PERFORMING ORGANIZATION REPORT NUMBER
9. SPONSORING/MONITORING AGENCY NAME(S) AND ADDRESS(ES)	10. SPONSOR/MONITOR'S ACRONYM(S)
	11. SPONSOR/MONITOR'S REPORT NUMBER(S)

12. DISTRIBUTION/AVAILABILITY STATEMENT
Approved for public release; distribution unlimited

13. SUPPLEMENTARY NOTES

14. ABSTRACT

15. SUBJECT TERMS

16. SECURITY CLASSIFICATION OF:			17. LIMITATION OF ABSTRACT	18. NUMBER OF PAGES	19a. NAME OF RESPONSIBLE PERSON
a. REPORT **unclassified**	b. ABSTRACT **unclassified**	c. THIS PAGE **unclassified**	**Same as Report (SAR)**	**9**	

APPROACH

The MTF, which is the magnitude of the Fourier transform of the PSF, was computed for two different water bodies using measurements of optical properties and analytical formulations described by Wells (1973) and Hou et al. (2007). The MTF of an aquatic medium, $H(\psi, z)$, can be represented by:

$$H(\psi, z) = e^{-D(\psi)Z}, \quad (1)$$

where Z is the range, $D(\psi)$ is the decay transfer function (DTF), and ψ is spatial frequency. By application of small-angle scattering approximations (Wells, 1973) the collimated DTF can be approximated as:

$$D^c(\psi) = c - S(\psi), \quad (2)$$

where c is the beam attenuation coefficient and $S(\psi)$ is the light scattered back into the acceptance cone:

$$S(\psi) = 2\pi \int_0^{\theta max} J_o (2\pi\theta\psi)\, \beta(\theta)\, \theta\, d\theta, \quad (3)$$

where $\beta(\theta)$ is the volume scattering function (VSF), θ is the scattering angle, and J_o is the zero-order Bessel function. The desired focused DTF can then be obtained by transformation in terms of spatial frequency ($2\pi\theta\psi$) (see Wells, 1973 for more details):

$$D(\psi) = \int_0^1 D^c(\psi\, t)\, dt. \quad (4)$$

In situations where the VSF may not be quantified, the following assumptions about the VSF have been made (e.g., Wells, 1973):

$$\beta(\theta) = (b\, \theta_o) / [2\pi\, (\theta_o^2 + \theta^2)^{3/2}], \quad (5a)$$

where θ_o is mean square angle and b is the scattering coefficient:

$$b = 2\pi \int_0^{\pi} \beta(\theta) \sin\theta\, d\theta; \quad (5b)$$

therefore a closed-form solution for the MTF is possible without direct measurements of the VSF:

$$D(\psi) = c - [b\, (1 - e^{-2\pi\, \theta o\, \psi})] / (2\pi\, \theta_o\, \psi). \quad (6)$$

The optical data necessary for MTF computations were collected from two field sites as part of the ONR sponsored RaDyO program: (1) Scripps Institution of Oceanography (SIO) Pier, a shallow-water, eutrophic environment and (2) the Santa Barbara Channel (SBC), a deeper, mesotrophic environment (Chang et al., 2010). The data processing and analysis approach utilized factory-recommended and published calibration and correction procedures for IOP sensors (e.g., Zaneveld et al., 1994; Pegau et al., 1997; Sullivan et al., 2006; Zhang et al., 2009). Profiler measurements were used to compute

optical products: backscattering ratio, $\tilde{b}_{bp}(\lambda) = b_{bp}(\lambda)/b_p(\lambda)$; the slope of the $c_p(\lambda)$ spectrum, γ, an indicator of particle size distribution (Boss et al., 2001); the real part of the index of refraction of particles, n_p, from γ and $\tilde{b}_{bp}(\lambda)$ (Twardowski et al., 2001), useful for obtaining information about the relative density of particles; the single-scattering albedo, $\omega_o = b / c$; and chlorophyll concentration (Chl) from chlorophyll fluorescence and spectral absorption using the methods of Sullivan et al. (2005). The MASCOT data were used to compute a "bubble index" (BI), where $BI = \beta(70°) / \beta(120°)$. This BI is based on theoretically computed VSFs of relatively large bubbles (> 10 μm), which show pronounced enhancement of the VSF between 60° and 80° (Czerski et al., in press; Twardowski et al., submitted manuscript). Hence, increases in the BI can be indicative of a relative increase in the concentration of larger bubbles.

Relationships between physical, hydrographic, and optical properties and the imaging performance parameter, MTF, were determined for the SBC experiment by use of wavelet analysis. Continuous wavelet transforms (CWTs), cross wavelet transforms (XWTs), and wavelet coherence (WTC) are useful tools for analyzing localized, intermittent oscillations in data series, as well as the relationship and linkages between two data series and the strength of the relationship(s) (see Grinsted et al., 2004). Fourier expansion (e.g., fast Fourier transform; FFT) has traditionally been the technique employed for determining the frequencies present in a signal. However, FFTs have only frequency resolution and no time resolution. In other words, although FFTs can reveal all frequencies present in a signal, they cannot determine when these frequencies are present in time. Similar to this, coherence analysis can be used to find common periodicities between two different time series; however, determined commonality is not localized in time or space. Wavelet analysis can be utilized to expand data series into time-frequency space and thus identify localized intermittent periodicities at multiple frequency and temporal resolutions.

WORK COMPLETED

Measured optical properties at 532 nm from SIO Pier and the SBC were used to compute the imaging performance parameter, MTF, at ranges set equal to the water depth. The MTF formulation presented by Wells (1973) (Eqs. 1-4) was utilized, with near-forward angle scattering provided by the LISST-100X. The β-approximation (Eq. 5) was evaluated using SIO Pier data by comparing the MTF computed using the LISST-measured near-forward angle scattering (θ between 0.05 and 8.25°) and the order zero Bessel function, J_o (Eq. 3) versus that computed using an approximated VSF (Eq. 5) and a mean square angle determined from LISST measurements (0.07 rad).

The β-approximation allowed us to perform a sensitivity analysis of particle concentration versus composition effects on the variability of the MTF in order to determine the relative importance of particle effects on the MTF. In the context of Eqs. 5 and 6, the particle composition effect is embodied in the mean square angle, θ_o. Particle concentration effects were explored by varying the beam attenuation coefficient, $c_{pg}(532)$, between 0.5 and 1.0 m^{-1} by steps of 0.1 m^{-1} while keeping the mean square angle, θ_o, constant at 0.07 rad, which is θ_o computed for the LISST measurements. The mean square angle was then varied between 0.03 and 0.19 rad by steps of 0.04 rad while keeping $c_{pg}(532)$ constant at 0.6 m^{-1} to investigate relative particle composition effects. Note that we are using variability in θ_o as a *proxy* for relative changes in particle composition. The range was set at 2 m and ω_o was 0.9 in both situations.

Relationships between the MTF and other parameters were quantified using a series of Morlet wavelets that were applied as band-pass filters to 2-m time series of the MTF, physical properties, and optical properties and products. The wavelets were stretched in time by varying their scale and normalizing them to have unit energy. The statistical significance of wavelet power was assessed for various properties to determine dominant scales of variability and the periods at which they occur (Grinsted et al., 2004). Periods and frequencies of high and significant wavelet power were interpreted as dominant modes of variability at specific times. XWTs and WTCs were applied to time series data to expose high common power and relative phase between two variables in time-frequency space. A Monte-Carlo test was performed to determine the statistical significance of the computed coherence. In addition to CWT, XWT, and WTC analysis for 2-m time series data, WTC methods were applied to depth-resolved profiles of physical and optical properties and the MTF. Using this method, common periodicities between two different parameters in vertical space were evaluated as a function of depth.

RESULTS

Variability of near-surface MTF at both field sites was strongly influenced by physical forcing – meteorological processes in the SBC and rip currents at SIO Pier. The 2-week SBC field experiment can be partitioned into three distinct periods: (1) diurnal winds (11 – 15 September), (2) persistent strong winds and upper water column mixing (15 – 18 September), and (3) an advection event characterized by relatively high Chl and elevated optical quantities (19 – 21 September) (Figure 1). During diurnal winds and the sustained strong wind event in the SBC, higher wind speeds were associated with particle characteristics indicative of larger, non-pigmented particles with higher relative indices of refraction and decreases in the MTF. The presence of larger particles with higher index of refraction observed during the high winds of the SBC RaDyO experiment could have been the result of wind-induced mixing of the upper water column waters and surface bubble injection or an increase in non-chlorophyll containing particles (perhaps minerogenic particles or senescent diatoms) or a combination of both of these factors. Anderson et al. (2008) and references therein have reported on phytoplankton succession in the SBC, with diatom dominance during upwelling periods (spring and summer), followed by continued surface depletion of nutrients and stratification, and likely diatom sinking in the autumn. It is possible that these senescent diatoms were retained in near surface waters during strong mixing associated with high winds.

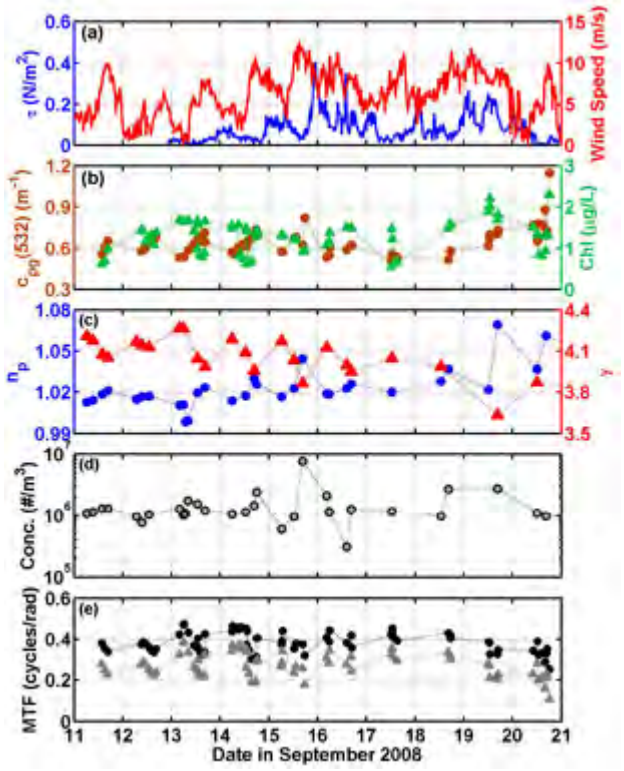

Figure 1. Time series of (a) wind stress (blue) and wind speed (red), (b) $c_{pg}(532)$ (brown dots) and Chl (green triangles) at 2 m, (c) near-surface n_p (blue dots) and γ (red triangles), near-surface (d) volumetric bubble concentration derived from BI, and (e) MTF for $\Psi = 3$ rad^{-1} (black dots) and $\Psi = 50$ rad^{-1} (gray triangles) calculated from 2 m optical data collected in the SBC.

Surface bubble injection is often associated with strong sustained winds, which in itself would result in substantive changes in particle composition characteristics in surface waters (Zhang et al., 2011). Information about bubble concentration was obtained from the BI, which was derived from the ratio of MASCOT-measured VSFs at 70° and 120°. The BI can be used as a proxy for the concentration of the large bubble subpopulation, following Twardowski et al. (submitted manuscript). The derived concentration of relatively large bubbles (> 10 µm in diameter) increased by nearly an order of magnitude on 15 September 2008 and by a factor of three on 18 September, coinciding with periods of sustained elevated wind speeds (Figure 1d). The increase in the concentration of the large bubble subpopulation was accompanied by a decrease in the slope of the particulate attenuation spectra, indicative of an increase in particle size (Figure 1c).

Although not statistically significant in 2-m time series data, the observed advection/bloom event starting on 19 September 2008 resulted in significant coherence between the MTF and the IOPs and IOP products indicative of particle concentration and composition at about 20-m water depth. This event was marked by a decrease in the MTF, increases in the magnitude of all IOPs, Chl, and n_p and a decrease in γ, indicative of an increase in the concentration of larger biogenic particles with relatively higher refractive index (Figure 1). The concentration of the large bubble subpopulation during this

time period was relatively low, suggesting lesser effects due to surface bubble injection and more to a phytoplankton bloom that was associated with a shift in the SBC circulation (Figure 1).

Highly reflective minerogenic particles with relatively high bulk particle index of refraction were associated with SIO Pier rip currents, which resulted in a large increase in the MTF. These particles, although not explicitly sampled or analyzed, appeared like mica flakes, which although rare in beach sand, have been observed along beaches in San Diego, CA. This increase in the MTF was likely due to enhanced reflectivity coupled with relatively high visibility; beam attenuation was not greatly elevated during the rip current event and Chl was at a minimum (Figure 2).

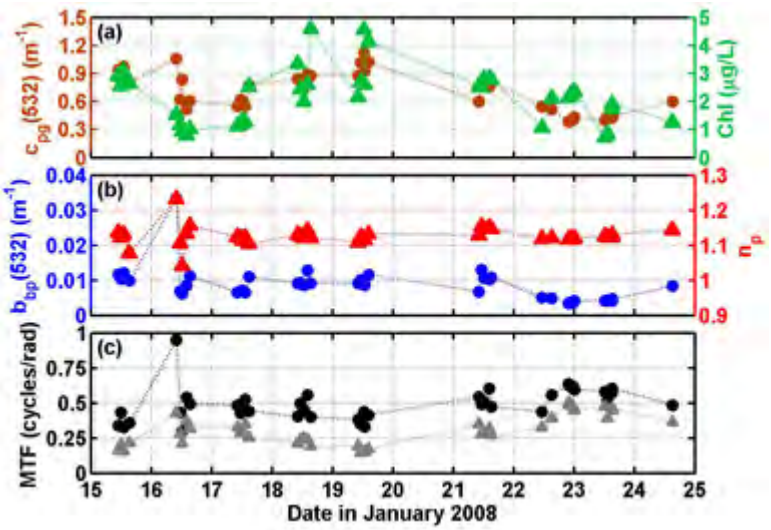

Figure 2. SIO Pier time series of 2-m (a) $c_{pg}(532)$ (brown dots) and Chl (green triangles) and (b) $b_{bp}(532)$ (blue dots) and n_p (red triangles); and (c) MTF ($\Psi = 3$ rad^{-1} in black dots and $\Psi = 50$ rad^{-1} in gray squares).

These observations are particularly interesting as one would expect the imaging performance parameter to be influenced primarily by particle concentration as revealed by the magnitude of IOPs; however we found that particle size and type (relative density information gained from the real index of refraction of particles) were important sources of variability in the MTF.

Our results show that the effects of particle composition on the shape of the VSF in the near-forward direction are important to imaging performance, which is a unique observation facilitated by advancements in *in situ* optical instrumentation. By performing a sensitivity analysis using the β-approximation formulation for the MTF, we were able to elucidate the relative importance of particle effects on the MTF (Figure 3). Results suggest that at θ_o between 0.07 and 0.11 rad, particle concentration and composition affected MTF variability similarly. At θ_o greater than 0.11 rad, MTF variability was stronger with variable IOPs, i.e. particle concentration effects dominated. Strikingly, when θ_o is between 0.03 and 0.07 rad (i.e. particle size distributions trending toward larger sizes), the MTF is much higher for frequencies less than 30 rad^{-1} (Figure 3). Here, particle composition effects dominated MTF variability, in a relative sense. For the specific ranges of variability in optical

properties we observed during the study, these modeling results are consistent with the strong coherence observed between particle composition parameters and imaging performance.

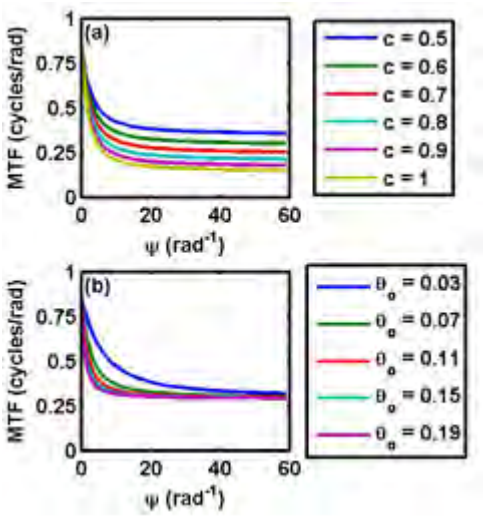

Figure 3. Particle concentration versus composition effects on MTF variability. (a) MTF computed by varying the beam attenuation coefficient, c (as indicated), while keeping the mean square angle, θ_o, constant at 0.07 rad. (b) MTF computed by varying θ_o (as indicated) while keeping c constant at 0.6 m^{-1}. The range was set at 2 m and ω_o was 0.9 in both situations.

The small-angle approximation (Eq. 5; e.g., Wells, 1973) assumes strong forward scattering, which was not the case during the SIO Pier rip currents. To explore this further, we evaluated MTFs computed from the DTF using measured β (Eq. 3) versus those calculated using approximated β (Eq. 6; θ_o = 0.07 rad) for the SIO Pier data set (Figure 4). The β-approximation method produced very similar MTFs to those computed using measured β, particularly at high spatial frequencies (> 10 rad^{-1}). MTFs at spatial frequencies less than 10 rad^{-1} were not comparable during periods when the backscattering coefficient exceeded 0.012 m^{-1}. Results from the two methods deviated greatly from each other at all spatial frequencies during the rip current event (Figure 4). Here, we show that in highly backscattering environments such as those with substantial minerogenic particles, the shape of the VSF cannot be assumed when computing imaging performance parameters such as the MTF.

IMPACT/APPLICATIONS

Optically-derived particle characteristics such as bulk particle index of refraction and particle size distribution were shown to be significantly related to the variability of the MTF. This, in addition to the great temporal variability in environmental conditions observed at two different field sites stresses the importance of obtaining or predicting optical properties and derived particle composition characteristics (describing relative particle size and type) at temporal and spatial scales necessary to quantify rapid changes in image processing parameters. Importantly, estimates of water clarity or turbidity are not the only factors influencing the variability of the image performance parameters, particularly at steep near-forward scattering angles, where variability in the MTF was found to be

dominated by particle composition effects. We also show that the standard approximation for the VSF cannot be used to compute imaging performance in environments with highly backscattering/reflective particles.

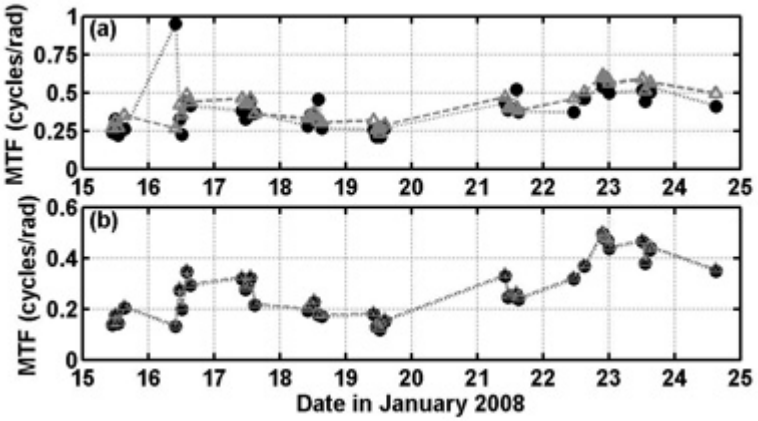

Figure 4. SIO Pier time series of MTF at Ψ = (a) 3 rad^{-1} and (b) 50 rad^{-1}, with MTFs computed using the β-approximation (e.g., Wells, 1973) shown with gray triangles.

RELATED PROJECTS

None.

REFERENCES

Anderson, C. R., D. A. Siegel, M. A. Brzezinski, and N. Guillocheau (2008), Controls on temporal patterns in phytoplankton community structure in the Santa Barbara Channel, California, *J. Geophys. Res.*, *113*, C04038, doi:10.1029/2007JC004321.

Boss E., M. S. Twardowski, and S. Herring (2001) Shape of the particulate beam attenuation spectrum and its inversion to obtain the shape of the particle size distribution, Appl. Opt., 40, 4885-4893.

Chang, G. and M. S. Twardowski (2011) Effects of physical forcing and particle characteristics on underwater imaging performance, J. Geophys. Res., in press.

Chang, G., M. S. Twardowski, Y. You, M. Moline, P.-W. Zhai, S. Freeman, M. Slivkoff, F. Nencioli, and G. W. Kattawar (2010) Platform effects on optical variability and prediction of underwater visibility, Appl. Opt., 49(15), 2784-2796.

Czerski, H., M. S. Twardowski, X. Zhang, and S. Vagle (2011) Resolving size distribution of bubbles with radii less than 30 microns with optical and acoustical methods, J. Geophys. Res., doi:10.1029/2011JC007177, in press.

Grinsted, A., J. C Moore, and S. Jevrejeva (2004) Application of the cross wavelet transform and wavelet coherence to geophysical time series, Nonlin. Proc. in Geophys., 11, 561-566.

Hou, W., Z. Lee, and A. D. Weidemann (2007) Why does the Secchi disk disappear? An Imaging perspective, Opt. Expr., 15, 2791-2802.

Pegau, W. S., D. Gray, and J. R. V. Zaneveld (1997) Absorption and attenuation of visible and near-infrared light in water: dependence on temperature and salinity, Appl. Opt., 36, 6035-6046.

Sullivan, J. M., M. S. Twardowski, P. L. Donaghay, and S. Freeman (2005) Using optical scattering to discriminate particle types in coastal waters, Appl. Opt., 44, 1667-1680.

Sullivan, J. M., M. S. Twardowski, J. R. V. Zaneveld, C. M. Moore, A. H. Barnard, P. L. Donaghay, and B. Rhoades (2006) Hyperspectral temperature and salt dependencies of absorption by water and heavy water in the 400-750 nm spectral range, Appl. Opt., 45, 5294-5309.

Twardowski, M. S., E. Boss, J. B. Macdonald, W. S. Pegau, A. H. Barnard, and J. R. V. Zaneveld (2001) A model for estimating bulk refractive index from the optical backscattering ratio and the implications for understanding particle composition in case I and case II waters, J. Geophys. Res., 106, 14,129-14,142.

Twardowski, M. S., X. Zhang, S. Vagle, J. Sullivan, S. Freeman, H. Czerski, Y. You, L. Bi, and G. Kattawar, The optical volume scattering function in the surf zone inverted to derive particulate sediments and bubble populations, (submitted manuscript).

Wells, W. H. (1973) Theory of small angle scattering, in AGARD Lec. Series No. 61, pp. 3.3.1 – 3.3.19, NATO, Neuilly-sur-Seine, France.

Zaneveld, J. R. V., J. C. Kitchen, and C. M. Moore (1994) Scattering error correction of reflecting-tube absorption meters, in Ocean Optics XII, J. S. Jeffe (Ed.), Proc. SPIE 2258, 44-55.

Zhang, X., L. Hu, and M-X. He (2009) Scattering by pure seawater: Effect of salinity, Opt. Expr., 17, 5698-5710.

Zhang, X., M. Twardowski, and M. Lewis (2011), Retrieving composition and sizes of oceanic particle subpopulations from the volume scattering function, *Appl. Opt.*, *50*, 1240-1259.

PUBLICATIONS

Chang, G., M. S. Twardowski, Y. You, M. Moline, P.-W. Zhai, S. Freeman, M. Slivkoff, F. Nencioli, and G. W. Kattawar (2010) Platform effects on optical variability and prediction of underwater visibility, Appl. Opt., 49(15), 2784-2796.

Chang, G. and M. S. Twardowski (2011) Effects of physical forcing and particle characteristics on underwater imaging performance, J. Geophys. Res., in press.